Jour. Korean Earth Science Society, v. 24, no. 1, p. 36–45, January 2003

On the Occurrences of Pyrrhotite from the Yeonhwa 1 Mine, Korea

Jae Il Chung and Young Up Lee*

Department of Earth & Environmental Sciences, College of Natural Sciences,
Chonbuk National University, Jeonju 561-756, Korea

Abstract : This study is made for examining the characteristics of the lead-zinc deposition from the mineralogy of pyrrhotite at the Yeonhwa 1 Mine, Korea. The pyrrhotite of the Yeonhwa 1 mine is divided two species; the pyrrhotites I and II. The pyrrhotite I that represents the product in Stage II mineralization is characterized by hexagonal pyrrhotite occurring as the mechanical mixtures of hexagonal and monoclinic phases with various proportion. These mixtures might be formed from "primary" hexagonal pyrrhotite by the subsequent retrograde reaction and/or by the influence of later mineralization in Stage III. Whereas the pyrrhotite II crystallized out in later Mineralization Stage III (hydrothermal stage) is always monoclinic variant with ferromagnetic properties; no two phase mixtures have been recognized.

Keywords : pyrrhotite, hexagonal, monoclinic, retrograde, Yeonwha 1

Introduction

In certain sulphide minerals, the variety closely related to superstructure is usually attributed to the ordered and partially ordered arrangement of metal vacancy. Pyrrhotite has long been known as one of such minerals. Pyrrhotite ($Fe_{1-x}S$) is a familiar mineral distributed widely in nature and occurs with varying amounts in many ore deposits of different genesis, and has been studied by many workers not only for natural minerals, but also for synthetic materials of the Fe-S system. As a result, it has been revealed that pyrrhotite has complex features in chemical composition, crystal structure and magnetic properties.

Up to date, about ten different structural variants for pyrrhotite have been found (Carpenter and Desborough, 1964; Morimoto and Nakazawa, 1968; Vorma, 1970; Morimoto *et al.*, 1975a, b). All, however, are modifications of the NiAs type structure, i.e., a superstructure of the NiAs type sub-cell ($\underline{A}$ = 3.45 Å and $\underline{C}$ = 5.8 Å with hexagonal symmetry), where A and C denote the dimensions of the elementary sub-cell, and in natural pyrrhotite the three low-temperature modifications have been distinguished by X-ray diffraction microscopic observation and electron microscopy. They are monoclinic pyrrhotite, 4C type; intermediate pyrrhotite, $\underline{n}$C type and hexagonal troilite 2C type; where $\underline{n}$ denotes the numbers of multiple of C-spacing of elementary sub-cell, having both rational and non-rational values for c-dimensions of the superstructure; i.e., $\underline{n}$ = 5, 5.5 or 11 and 6 or 12, and $\underline{n}$ = non-rational number ranging from 4.8 to 6.2.

The 4C type pyrrhotite ($\underline{a}$ = 11.885 Å, $\underline{b}$ = 6.870 Å, $\underline{c}$ = 22.80 Å, $\beta = 90°47'$, $\underline{c}$ = 4C) and the 2C type troilite ($\underline{a}$ = 5.976 Å, $\underline{c}$ = 11.60 Å, $\underline{c}$ = 2C) are stoichiometric with the composition Fe_7S_8 ($Fe_{0.875}S_{1.00}$, $\underline{x}$ = 0.125, atomic percent Fe: 46.67) and FeS ($\underline{x}$ = 0.00, atomic percent Fe: 50.00), respectively, whereas the $\underline{n}$C type pyrrhotite is nonstoichiometric with the composition from approximately Fe_9S_{10} ($Fe_{0.90}S_{1.00}$, $\underline{x}$ = 0.10, atomic percent Fe: 47.37, $\underline{n}$ = 5) to $Fe_{11}S_{12}$ ($Fe_{0.99}S_{1.00}$, x = 0.01, atomic percent Fe: 47.83, $\underline{n}$ = 6) and is apparently orthorhombic, though real symmetry is monoclinic (Morimoto *et al.*, 1970; Nakazawa and Morimoto, 1971; Morimoto *et al.*, 1975b). The Fe-deficient intermediate phases belonging to the $\underline{n}$C type transform into a high-temperature phaes, $\underline{n}$A, above 220°C (Nakazawa and Morimoto, 1971).

The intermediate phases belonging to the $\underline{n}$C

*E-mail: yulee@moak.chonbuk. ac.kr

type have been considered to have a hexagonal symmetry and called "hexagonal pyrrhotite" for a long time. Strictly speaking, the usage of the term "hexagonal pyrrhotite" at present is not appropriate in view of the recent works by Morimoto *et al.* (1975a, b) as noted before. In the present paper, however, following a long tradition in the field of sulphide mineralogy, the term "hexagonal pyrrhotite" is used to the nC type pyrrhotite for convenience and "monoclinic pyrrhotite" denotes the 4C type pyrrhotite. Accordingly hkl indices for the nC type pyrrhotite here used are based upon the hexagonal structure cell. With respect to magnetic properties, the hexagonal pyrrhotite is anti-ferrimagnetic (Haralden, 1941), while the monoclinic pyrrhotite is ferromagnetic (Byström, 1945) at a room temperature.

On the X-ray diffraction patterns of pyrhotite, sharp and symmetrical 10.2 superstructure reflection is indicative of troilite or hexagonal pyrrhotite. Distinction between troilite and hexagonal pyrrhotite is possible from the difference in the spacings of the 10.2 superstructure reflections; $\underline{d} = 2.093$ Å and 2.07~2.0587 Å, respectively (Arnold, 1962). Two reflections (202 and $20\bar{2}$) with approximately equal intensity and a angular aperture of 0.35 ($\Delta 2\theta$ for FeKα) indicates monoclinic pyrrhotite (Arnold, 1962). The 202 reflection overlaps with the 10.2 superstructure reflection of hexagonal pyrrhotite. Accordingly, the $20\bar{2}$ reflection indicates the presence of monoclinic pyrrhotite in the two-phase mixture.

On the other hand, there are two effective methods to distinguish the monoclinic pyrrhotite from hexagonal pyrrhotite in the polished sections. One is a structural etching by saturated chromic acid (Arnold, 1962) and hydrogen iodide (Schneiderhöhn, 1952), in which the monoclinic phase of pyrrhotite is etched more strongly than the hexagonal phase. The other is a magnetic staining with Bitter's colloidal suspension method using magnetic colloid (Bitter, 1931), in which magnetic domain structures appear only within the monoclinic pyrrhotite, which is ferrimagnetic. Magnetite colloid may be obtained by the precipitation with KOH from an equimolar solution of ferro-and ferric-chlorides. The black magnetite precipitate is washed and suspended in a 0.5 percent soap solution. The Bitter's suspension has previously been used in the study of the magnetic domain structure of iron.

Recent improvements of electron microprobe, in particular the success in minimizing the spot size of electron beams on the specimen surface less than 1 μmΦ, together with the high-contrast technique permit the observation of the minute minerals distinguishable from others in the back-scattered electron images. Generally, in the back-scattered electron images, when topographic effects on the specimen surface are negligible, the brightness of a given phase in the phase assemblages increases with increasing the average atomic number, $\underline{Z}$, which is a suitable parameter for the chemical contrast. From the definition, the $\underline{Z}$ is written as $\Sigma C_i Z_i$, where C_i and Z_i respectively refer to the weight fraction (mass concentration) and atomic number of element i contained in the phase. By means of the simple calculation, we may obtain the average atomic numbers for the two phases in pyrrhotite; hexagonal pyrrhotite: $\underline{Z} = 22.10$~22.15, monoclinic pyrrhotite: $\underline{Z} = 22.03$.

The textural relationships between hexagonal and monoclinic pyrrhotite in the two-phase intergrowth in ores have been studied by many investigators (e.g., Park and Miyazawa, 1971; Mariko *et al.*, 1974; Muramatsu and Nambu, 1975; Miyazawa, 1977; Sugaki *et al.*, 1978). Summarizing the data given by previous workers, the mode of formation of monoclinic pyrrhotite may be ascribed to the following four possibilities; (1) exsolution from hexagonal pyrrhotite by the cooling during the subsequent period of mineralization, (2) oxidation of hexagonal pyrrhotite, (3) hydrothermal sulphidation of hexagonal pyrrhotite with increasing sulphur fugacity, and (4) primary crystallization. These characteristics of the occurrences of pyrrhotite are deeply related with the ore depodition. This

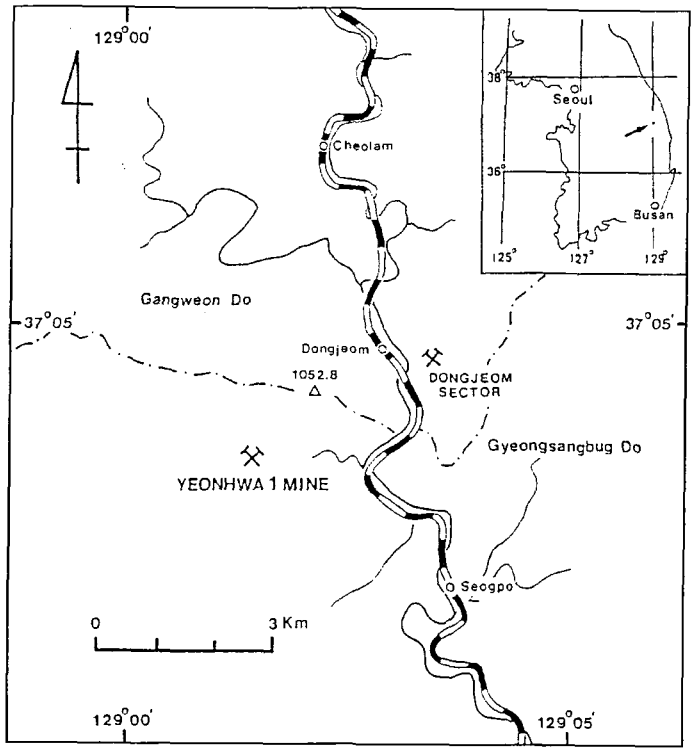

Fig. 1. Map showing the location of the Yeonhwa 1 Mine district.

study is made for examining the characteristics of the lead-zinc ore deposition from these various mineralogy of pyrrhotite at the Yeonhwa 1 Mine. Korea.

Location and Geologic Settings

The Yeonhwa 1 mine lies about 5 km north of Seogpo station on the Ryeongdong Line of the Korean National Railway, and the mine Province, approximately at lat. 37°04 N and long. 129°02 E (Fig. 1). In the mine area, the basement rocks of Precambrian granite gneisses - "Taebaegsan Gneiss Complex" (Lee and Kim, 1984) and the overlying Cambro-Ordovician sedimentary rocks of the Joseon Supergroup are exposed extensively. The results of K/Ar radiometric dating on three members of the gneiss complex given by Yun and Silberman (1979) are as follows; Dongjeom gneiss: 1,744 ± 52 Ma on Muscovite, pegmatite in Dongjeom gneiss: 1,754 ± 53 Ma for muscovite, and Hongjesa granite: 730 ± 22 Ma on biotite. This indicates that at least two phases of Precambrian intrusive and/or metamorphic events took place in the district.

The Cambro-Ordovician sediments belonging to Duwibong (platform) sequence have been divided into the following nine formations in ascending order (Cheong, 1969); the Jangsan Quartzite and the Myobong Slate; the Poongchon and the Hwajeol Formation; the Dongjeom Quartzite, the Dumudong and the Magdong Formation; and Jigunsan Slate and Duwibong Limestone. The boundary of Cambrian and Ordovician has been defined at the base of the Dongjeom Quartzite for convenience, though the biostratigraphic boundary lies at the upper horizon of the Hwajeol Formation (Kobayashi, 1953). Stocks of dykes of lamprophyre (K/Ar age: 213 4 Ma on muscovite; Yun and Silberman, 1979) have intruded into the above basement rocks and the sedimentary rocks of the Samcheog Group. Dykes of quartz-monzonite por-

phyry and diabase of unknown age also crop out in some places.

Structurally, the Yeonhwa 1 mine area occupies the eastern segment of the southern limb of Hambaeg syncline (called Baegunsan syncline by some authors), whose axis trending approximately EW~NW and plunging westwards. The structure of strata on the surface in the mine area is fairly steep; they strike NE and dip between 40° and 60° NW in general, however, in the underground dips become gentle, from 25° to 30° NW. In some places, the strata have been overturned due to local disturbance of faultings. Minor foldings and warpings are developed locally. The dominant faults in the mine area include (1) steep reverse fault of EW strike with a steep dip of about 60° in north of the mine workings, that places the Pungchon Limestones over the Hwajeol Formation, (2) steep reverse fault trending NS~N30°E dipping SW, and (3) steep reverse fault striking N20~30°W with dips of 45°~85°W-SW.

Outline of the Ore Deposits

The zinc-lead calcic skarn deposits in the main mineralized tracts at Yeonhwa 1 are represented by several orebodies, showing lenticular and pipe-like shape and numerous veins. Of them, the large-scale orebodies exhibit a stratal form and pipe-like morphology, which have been controlled structurally by the intersections of NNE- and NNW- trending faults within the Pungchon Limestone, or by the intersections of these faults with the lithologic contact between the Myobong Slate and the overlying Pungchon Limestone (Daegi Limestone).

The mineralized zone of Dongjeom sector is located about 3 km northeast of the main mineralized tract. In this sector, the ore deposits include West, East and Dongjeom fault orebodies. The structural features as related to ore emplacement of the West and East orebodies with skarn type are quite similar to those of the Bonsan ore deposits. However, the latter has been emplaced along the dyke of quartz-monzonite porphyry, which intruded into the Dongjeom fault trending NS direction and dipping steeply eastwards.

Occurrence and Optical Properties

Summarizing the informations on skarn deposits in Republic of Korea and Japan, Miyazawa (1976) has already stated that pyrrhotite is usually predominate in amounts as compared with pyrite. In Korea, except for ore deposits of the Ulsan and Mulkum mines, where sulphide minerals are rather minor, almost all of the ore deposits are characterized by the abundance of pyrrhotite.

In the case of the Yeonhwa 1 zinc-lead (-silver) ores, pyrrhotite is one of the commonest and the most abundant ore-forming metallic minerals. Also vertical zoning of ore minerals is distinct in the mine, and pyrrhotite tends to increase with increasing depth. As for the features of metallic mineraizations in calcic Fe, Cu, Zn-Pb, W and Mo skarn deposits in Japan and Korea, Miyazawa (1976) has stated that the ore deposits have three stages in time evolutionary trend; Stage I: oxide stage, Stage II: sulphide stage (1), and Stage III: suphide stage (2). And in the study on the calcic Zn-Pb skarn deposits of the Chichibu mine, Japan, Park and Miyazawa(1971) have divided the Stage II into the two substages: Stage IIa and IIb on the basis of sulphide mineralogy on pyrrhotite. The Yeonhwa 1 pyrrhotite also shows this time evolutionary trend of ore deposition and may also be divided largely into two species on the basis of the paragenetic sequence in the course of metallic mineralization. They are (1) earlier pyrrhotite and (2) later pyrrhotite, which may be respectively denoted as pyrrhotite I and pyrrhotite II, hereinafter.

The pyrrhotite I represents the major constituent of the ores and is closely associated with sphalerite, pyrite, galena and arsenopyrite, and on some occasions with magnetite. The mineral occurs as grains with irregular shape, usually from 200 μm to

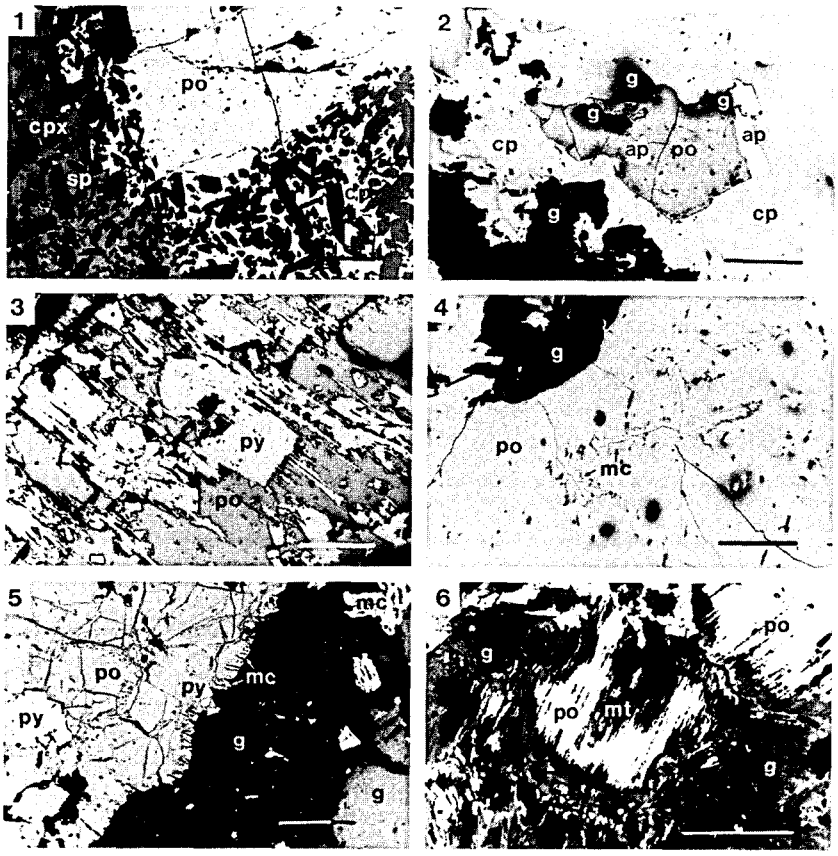

Fig. 2. Photomicrographs of the polished sections (one polar), showing the mode of occrrence of pyrrhotite. Bar scale indicates 100 in length. Abbreviation: po=pyrrhotite. cpx=clinopyroxene. sp=sphalerite. cp=chalcopyrite. g=galena. ap=arsenopyrite. py=pyrite. mc=marcasite.

more than several millimeters across. The pyrrhotite II, on the other hand, occurs as a minor constituent of the later vein deposits and is closely associated with sphalerite, galena, pyrite and rhodochrosite. The mineral is anhedral in form, ranging from 20 to 500 μm across in size. Also, the mineral occurs as independent grains, ranging in size from 20 to 50 μm across within gangue minerals, mostly calc-silicates, and it is trace in amounts.

On some occasions, grains of pyrrhotite I are partly replaced by marcasite along its fractures and cleavage cracks, especially in the ore containing bismuth minerals, producing lamellae of marcasite with parallel arrangement (Fig. 2(5)). According to Edward (1954), the formation of marcasite from pyrrhotite depends upon the subsequent change of redox potential and temperature of residual ore-forming fluids during the course of pyrrhotite to marcasite has often been pointed out by a number of the iron sulphides in the atmospheric weathering, and supergene alteration of pyrrhotite to marcasite has often been point out by a number of investigators (e.g., Ramdohr, 1980). However, in the present case, it is difficult to ascribe the marcasite to the product of supergene alteration, and it may be appropriate to prefer the hypogene origin, because of its occurrence at large depth.

The pyrrhotite I is often altered to the delicate myrmekitic intergrowths of pyrite and magnetite. This may be explained by the oxidation reaction as expressed by the following equation;

$$6FeS + 2O_2 = Fe_3O_4 + 3FeS_2 \quad (1)$$

Under the ore microscope, the Yeonhwa 1 pyrrhotites have the optical properties, which are identical with these described in literatures (e.g., Ramdohr, 1980; Edward, 1954). No internal structures within single grains have been confirmed by ordinary ore microscopy. The mode of occurrence of the pyrrhotite is shown in the photomicrographs illustrated in Fig. 2.

Chemical Composition

The determination of chemical composition of pyrrhotite with electron microprobe is encountered with some difficulty to elevate the accuracy even at the present analytical level. It has already been pointed out by several investigators that the precision of the analytical results for sulphides and sulphosalts with microprobe depends significantly upon the adequate choice of the standards utilized. In particular, pyrrhotite is more sensitive mineral to this respect than others, and it is insisted that microprobe analysis of pyrrhotite requires the use of standards which closely approximate the composition of the unknown.

On the other hand, X-ray diffraction methods, although more labourous, still provide more precise analyses for hexagonal pyrrhotite. Arnold (1958) has demonstrated for the first time that $\underline{d}_{102}$-spacing of hexagonal pyrrhotite is a sensitive indicator of its iron content, as far as the combined concentration of nickel, cobalt and copper in solid solution is less than 0.6 weight percent (Arnold and Reichen, 1962). At present the following equation representing calculated determinative curve for hexagonal pyrrhotite given by Yun and Hall (1969) is commonly used, in which they have selected previous data plus a few points of their own and normarized them all to $\underline{a}_0 = 5.4306$ Å for silicon standard.

$$\text{Atomic percent Fe} = 45.212 + 72.86\,(\underline{d}_{102} - 2.0400) + 311.5\,(\underline{d}_{102} - 2.400)^2$$
$$[\text{e.s.d.}] = 0.06 \quad (2)$$

The above methods do not apply to monoclinic pyrrhotite which has two peaks at the location of the 102 reflection of hexagonal pyrrhotite. However, the monoclinic pyrrhotite can be isochemically converted into hexagonal pyrrhotite by its heat treatment in an evacuated silica tube at 325°C for 3 to 5 minutes and rapidly quenching (Yun and Hall, 1969).

In the present study, electron microprobe analyses for pyrrhotite from the Yeonhwa 1 mine were

Table 1. Comparison of chemical composition of pyrrhotite by electron-microprobe analyses with those by x-ray diffraction.

Specimen	EPMA		X-ray
	mean	range	diffraction
	atomic percent Fe		atomic percent Fe
YH84-301	47.66	47.49~47.78	47.56
YH84-302	47.85	47.51~48.02	47.54
YH84-303	47.53	47.19~47.71	47.45
YH84-304	47.09	46.92~47.30	47.55
YH84-305	46.56*	46.47~46.70	
YH84-305	47.28	47.14~47.40	47.42
YH84-306	46.76*	46.50~47.04	
YH84-308	46.75*	46.32~46.36	
YH84-308	47.29	47.18~47.44	
YH84-309	46.34*	46.32~46.36	
YH84-309	47.27	47.01~47.41	47.35
YH84-310	46.59*	46.45~46.73	
YH84-310	47.16	47.10~47.19	47.38

Asterisk represents monoclinic pyrrhotite.

carefully carried out, using synthetic troilite as standard and low accelerating voltage of 15 kV, although Desborough *et al.* (1971) have recommended lower accelerating voltage of 6 kV in doing sulphur analyses. In Table 1, the results of the present microprobe analyses for iron are compared with those obtained by X-ray diffraction methods using Eq (2). There are some discrepancies between the two.

X-ray Diffraction

X-ray diffraction study on the Yeonhwa 1 pyrrhotites was carried out with FeK α-radiation ($\lambda K_\alpha = 1.9373$ Å) using X-ray diffractometer. The powder patterns in the narrow spans in the front region $2\theta = 58\sim54^\circ$ (FeK_α) were recorded at a slow scanning speed of 0.25 per minute. The patterns of the pyrrhotite I show a reflection at 2.066 Å with or without a shoulder at 2.051 Å of variable intensities, indicating that the materials are mechanical mixtures of hexagonal pyrrhotite (abbreviation: hpo) and monoclinic pyrrhotite (abbreviation: mpo) with various proportions. Also, in rare cases, some patterns show two reflections of approximately equal intensities at 2.057 Å and 2.051 Å, which suggest that the materials are consists almost entirely of mpo. On the other hand, the patterns of the pyrrhotite II always shows two reflections with equal intensities at 2.057 Å and 2.051 Å, indicating that the materials are represented by the single phase (mpo). X-ray diffraction patterns, showing the above noted features are reproduced in Fig. 3.

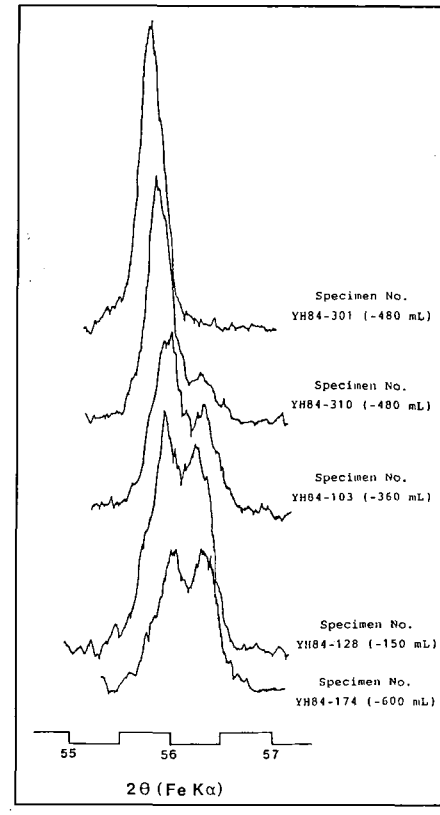

Fig. 3. X-ray diffraction patterns in the 2 region from 55° to 57° (Fe K) for pyrrhotites from Dongjeom sector.

Intergrowth Textures of the Two Phase Mixtures

In order to reveal the internal textures, particularly the fine intergrowth textures of hpo and mpo in the pyrrhotite I, the following three procedures were employed; (1) structural etching by saturated chromic acid, (2) Bitter's colloidal suspension method using a magnetite colloid, and (3) observations of back-scattered electron (compositional) images obtained by electron microprobe.

Structural etching by saturated chromic acid has already been applied to distinguish the two phases, hpo and mpo by some investigators and the good results are obtained (e.g., Miyazawa, 1976). Unfortunately, this technique was not always available in the present study. However, Bitter's colloid suspension technique has brought about the excellent results. As shown in Fig. 4, mpo phase is indicated by the lamellae of magnetic domain stained by magnetite colloids. As shown in Fig. 4 the texture of hpo in which lamellae of mpo, 50~100 μm long and less than 5 μm wide, are arranged with preferred orientation, are commonly observed. The direction of elongation of lamellar mpo is approximately equal within single grains. However, with increasing mpo, the lamellae gather and as a whole

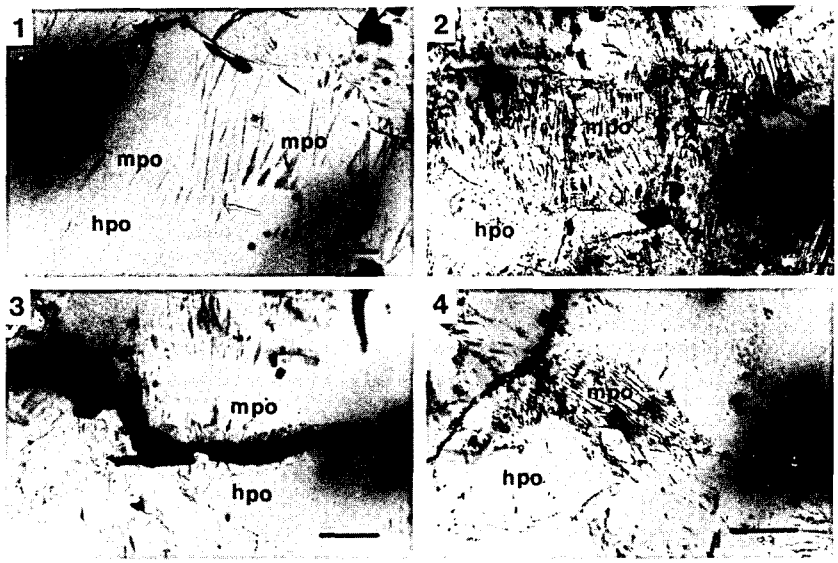

Fig. 4. Photomicrographs of the polished sections etched by magmatic colloid (one polar), showing the mode of occurrence of pyrrhotite. Bar scale indicates 100 in length. Abbreviation: hpo = hexagonal pyrrhotite. mpo = monoclinic pyrrhotite.

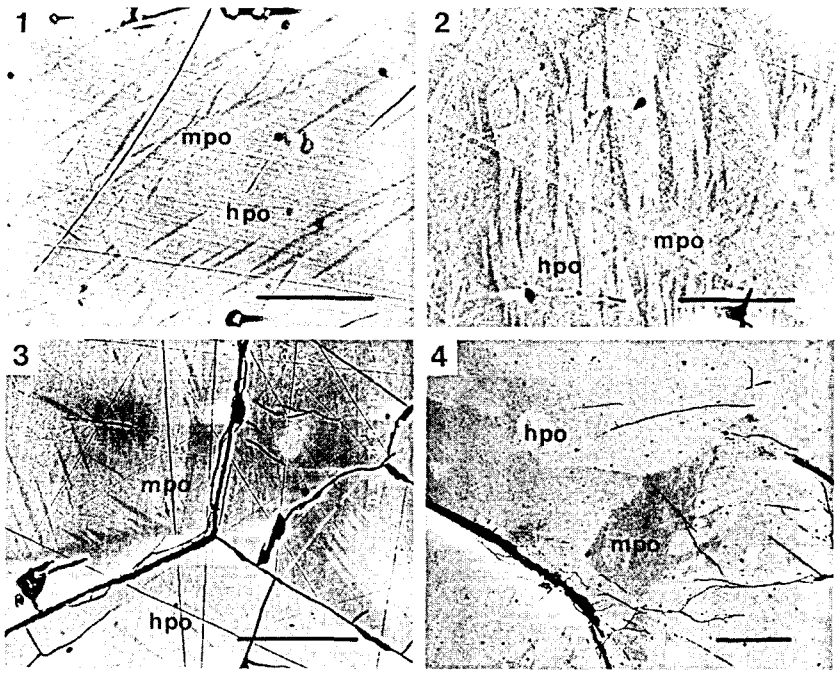

Fig. 5. Back-scattered electron (compositional) image showing the delicate intergrowth of monoclinic phase with hexagonal phase of pyrrhotite. Bar scale indicates 100 in length. Abbreviation: hpo = hexagonal pyrrhotite. mpo = monoclinic pyrrhotite.

the aggregates of mpo show irregular shape. With more increasing mpo, the final stage of the alteration show the small relicts of hpo scattering within the mpo base.

The alteration of hpo into mpo is also recognizabel along the grain boundary of hpo or along cleavage, microcraks or the penetrated calcite veinlets. The contrast of brightness with subtle differ-

ence in average atomic number Z between hpo and mpo is well exhibited in the back-scattered electron image as shown in Fig. 5. It is now apparent that the observations of back-scattered electron images are powerful tool to distinguish these two phases.

Conclusions

In the present work, it is revealed that the pyrrhotite of the Yeonhwa 1 mine may be divided largely into two species; i.e., the pyrrhotites I and II. The pyrrhotite I that represents the product in Stage II during the course of mineralization is characterized by hexagonal pyrrhotite occurring as the mechanical mixtures of hexagonal and monoclinic phases with various proportion. These mixtures might be formed from "primary" hexagonal pyrrhotite by the subsequent retrograde reaction and/or by the influence of later mineralization in stage III.

Whereas the pyrrhotite II crystallized out in later stage III (hydrothermal stage) is always monoclinic variant with ferromagnetic properties; no two phase mixtures have been recognizable. However, the study on the Yeonhwa 1 pyrrhotite that is one of the most important ore-forming metallic minerals is still meagre. In particular, further investigation of the mineral in relation to the time-evolutional trend during metallic mineralization is needed.

References

Arnold, R. G., 1958, The Fe-S system. Journal of Solid State Chemistry, 57, 218.

Arnold, R. G., 1962, Equilibrium relations between pyrrhotite and pyrite from 325°C to 743°C. Economic Geology, 57, 72-90.

Arnold, R. G. and Reichen, E., 1962, Measurement of metal content of naturally occurring, metal deficient, hexagonal pyrrhotite by an X-ray spacing method. American Mineralogist, 47, 105-111.

Bitter, F., 1931, In homogeneities in the magnetisation of ferromagmatic materials. Physics Review, 38, 1903-1905.

Byström, A., 1945, Monoclinic magnetic pyrrhotite. Arkiv Kemi, Mineral Geology, 19B, 1-8.

Carpenter, R. H. and Desborough, G, A., 1964, Range in solid solution and structure of natural occurring troilite and pyrrhotite. American Mineralogist, 49, 1350-1365.

Cheong, C. H., 1969, Stratigraphy and paleontology of the Samcheog Coalfield, Gangwon-do, Korea (1) (in Korean with English abst.). Journal of Geological Society of Korea, 5, 13-56.

Desborough, G. A., Heider, R. H. and Cwamanske, G. K., 1971, Improved quantitative electron microprobe analysis at low operating voltage. II. Sulfur. American Mineralogist, 56, 2136-2141.

Edward, A. B., 1954, Texture of the ore minerals and their significance. Australian Institute of Mineral and Metallurgy.

Haralden, H., 1941, Über die eisen (II) sulfide Mischkristalle. Zeitschrift Anorganic Chemistry, 246, 169-194.

Kobayashi, T., 1953, The Cambro-Ordovician Formations and Faunas of Chosen, pt. 4, Geology of South Korea with special reference to the Limestone Plateau of Gangwon-do (Kogendo). Imperial University of Tokyo Faculty Science Journal, Sector 2, 8, pt. 4, 145-293.

Lee, S. M. and Kim, H. S., 1984, Metamorphic Studies on the so-called Yulri and Wonnam Groups in the Mt. Taebaeg Area (in Korean with English abst.). Journal of Geological Society of Korea, 20, 195-214.

Mariko T., Imai, N. Shiga, Y. and Ichige, Y., 1974, Studies of the sulfosalts of copper VII. crystal structure of the exolution products $Cu_{12.3}Sb_4S_{13}$ and $Cu_{13.8}Sb_4S_{13}$ of unsubstituteed synthetic tetrahedrite. Canadian Mineralogist, 17, 619-634.

Miyazawa, T., 1976, Contact-metasomatic deposits in Japan and Korea. In Studies of Contact-metasomatic deposits. A3-A149.

Miyazawa, T., 1977, Contact-metasomatic deposits in Japan and Korea, in Miyazawa, T., ed., On the contact metasomatic deposits (in Japanese). Tokyo, Tokyo University of Education, A1-A146.

Morimoto N., and Nakazawa, H., 1968, Pyrrohotites: synthetics having two new superstructure. Science, 1, 161, 575-579.

Morimoto, N. and Nakazawa, H., 1970, Pyrrohotites: stochiometric compounds with composition $F_{3n-1}S_n(n>8)$. Science., 168, 964-966.

Morimoto, N., Gyobu, A., Mukaiyama, H. and Izawa, M., 1975a, Crystallography and stability of pyrrhotite. Economic Geology, 70, 824-833.

Morimoto, N., Nakazawa, H. and Watanabe, E., 1975b, Superstructure and non-stochiometry of intermediate pyrrhotite. American Mineralogist, 60, 240-248.

Muramatsu, Y. and Nambu, M., 1975, Mineralization of

Pyrrohotite at the Yaguki mine, Fushima Prefecture, Japan (in Japanese). In Nambu, M and Yamaoka, K., (eds.), Memorial Volume, Prof. Tsunehiko Takeuchi. Sendai, Tohoku University, 151-161.

Nakazawa, H. and Morimoto, N., 1971, Phase relations and superstructures of pyrrhotite, $Fe_{1-x}S$. Material Research Bulletin, 6, 345-358.

Park, H. I. and Miyazawa, T., 1971, On the pyrrhotite from the Chichibu Mine, Saitama Prefecture, Japanese Mining Geology, 21, 259-273.

Ramdohr, P., 1980, The ore minerals and their intergrowths. Pergamon Press, 2nd ed, 1206 p.

Schneiderhöhn, H., 1952, Lehrbuch der Erzlagerstaltenkunde, gustav fischer.

Sugaki, A. Shima, H., Kitakaze, A., Harada, H., 1978, Isothermal phase relations in the system Cu-Fe-Sn-S system (VI) (abst. in Japanese). Coll. Abst. Autumn Joint Meet., Mineralogical Society of Japan, Society of Mining Geologists of Japan and Japanese Mineralogy, Petrolology and Economic Geology, C-7, 106 p.

Vorma, A., 1970, Pyrrhotite-troilite intergrowth from Luikonahti copper deposit eastern Finland. Bulletin of Geology Finland, 42, 3-12.

Yun, S. K., and Silberman, M. L., 1979, K-Ar geochronology of igneous rocks in the Yeonhwa-Ulchin zinc-lead district and southern margin of the Taebaegsan basin, Korea. Journal of Geological Society of Korea, 15, 1013-1032.

Yund, R. A. and Hall, H. T., 1969, The miscibility gap between FeS and $Fe_{1-x}S$. Material Research Bulletin, 3, 779-794.

Manuscript received, July 15, 2002
Revised manuscript received, August 10, 2002
Manuscript accepted, August 20, 2002